

## INVESTIGATION OF FORCED CONVECTION HEAT TRANSFER FROM A BLOCK LOCATED IN A SQUARE CAVITY WITH ROTATING CYLINDERS

Meenakshi Sundar KANNAN<sup>a\*</sup>, Manikandan GURUNATHAN<sup>a</sup>, Rajesh KANNA P.<sup>b</sup>,

<sup>a</sup> Velammal College of Engineering and Technology, Madurai – 625009, India

<sup>b</sup> Al Ghurair University, Dubai, UAE.

\* Corresponding author; E-mail: meenakshisundark@gmail.com

*The influence of non-dimensional rotational velocity and horizontal rotating cylinders has drawn the interest of researchers for many years due to its importance in many applications. These cylinders are positioned in a square cavity which contain of a square block at the midpoint. The rotary horizontal cylinder subject to persistent heat flux boundary condition and square block at constant temperature condition is numerically studied. The numerical simulations have been conducted using commercial Computational Fluid Dynamics platform CFX available in ANSYS Workbench.. Results are obtainable for the non-dimensional rotational velocity  $\alpha$  ranging from 0 to 4 and for various direction of rotation of cylinders. The rotating effects results in decrease in heat transfer compared to heat transfer from fixed heated cylinder due to thickening of boundary layer as consequence of the rotation of the cylinder. Heat transfer rate increases with increase in Prandtl number of the fluid. The results are found to be in worthy agreement with existing targeted benchmark results. It was found that the dynamics and the structure of the primary vortex and the corner vortices were strongly affected by the Reynolds number. The analysis clearly defines that increasing Reynolds number the overall drag coefficient decreases, similarly the value of average Nusselt number also increases with an increasing Reynolds number for all the values of different rotating blocks under studied. The study exposes that important flow physics such as flow separation, boundary layer and recirculation. The results will be positive for similar condition occur in many industrial problems.*

Keywords: Staggered Cavity, Drag, Nusselt Number, Reynolds Number.

### 1. Introduction

Fluid flow and heat transfer in a cavity has drawn the interest of researchers for many years due to its importance in many applications [1]. These applications include microchip cooling, lubricating application, nuclear reactors, gas turbine channel flow, solar power collectors, furnace, drying technology, etc. [2]. The flow of liquids past heated fixed horizontal rounded cylinder(s) is a challenging conventional problem in fluid mechanics and heat transfer [3,4]. Heat transfer from a stationary flat cylinder has been a subject of interest for many experimental and theoretical researcher because of its many engineering applications. Dennis et al. [4] numerically investigated steady state laminar forced convection from a circular cylinder at low Reynolds numbers. The flow and energy equation were resolved for Prandtl number up to  $3.3 \times 10^4$  and Reynolds number up to 40 for the cylinder exposed to constant temperature. The predicted mean and local Nusselt number was associated with the available experimental data of McAdams [5] and Van Der Hegge Zijen [6] are found to approve with them. A numerical model was developed by Chun and Boehm [7] to study the forced convection heat transfer over a circular cylinder in cross flow. Two different cases were analyzed viz. cylinder surface subjected to constant heat flux and continuous wall temperature.

The advanced numerical model were able to successfully predict the heat transfer rate from the cylinder for Reynolds number up to  $Re = 2000$ , which were in good arrangement with the laboratory experimental values. They also stated that unchanging heat flux condition displayed a higher value of heat transfer coefficient at the constant wall temperature of the cylinder for the similar Reynolds number. Experiments were performed by Sanitjai and Goldstein [8] to investigate the heat transfer by forced convection from a circular cylinder in cross flow for Reynolds number  $2 \times 10^3$  to  $9 \times 10^4$  and Prandtl number from 7 to 176. The cylinder was subject to constant heat flux boundary condition. The study reported that on the front part ( $0^\circ < \theta < 85^\circ$ ) of the cylinder, local heat transfer upsurges with increasing Prandtl number. However, on the rear part ( $85^\circ < \theta < 180^\circ$ ), local heat transfer be contingent on flow characteristics near the surface.

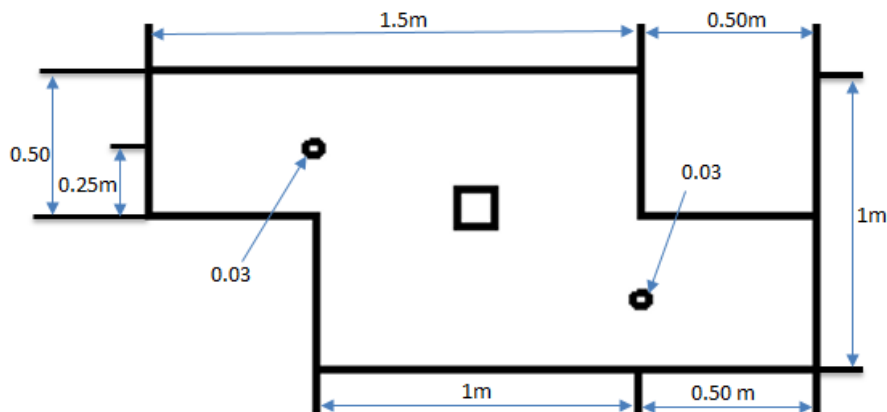


Fig 1. Schematic diagram of the Problem

## 2. Problem Statement and Mathematical Formulation

The numerical analysis of the problem has been performed using commercial computational fluid dynamics package CFX available of ANSYS Workbench 19 [14]. The cylinders at inlet and outlet are modeled as a wall subjected to rotation and constant heat flux. The block is subjected to isothermal condition. The region between the cylinder, square block and parallel plates is modeled as fluid. Simulations have been performed for different direction of rotation of inlet and outlet cylinders. For each fluid simulations have been performed for  $\alpha = 0, 1, 2, 3$  and 4. The Reynolds number considered in the study is less than 40. It is noticed that as reported by Bharti et al. [10] for  $Re < 49$  the flow can be treated as steady, incompressible and laminar.

Description of our problem in two dimensional measured in that a square cavity is considered with an aspect ratio of 1 ( $AR = H/L = 1$ ). Aspect ratio is the ratio of Length (L) to the Height of the cavity (H). The inlet is a protruded section at the top part of the left wall which has a length of 0.5L and breadth of 0.5L. The outflow is a protruded section taken at the bottom of the right wall which has a length 0.5L and breadth of 0.5L. In this problem the length and height of the cavity is taken as 1metre. A square block of side 0.1L is considered at the geometric midpoint of the cavity. Each cylinder is located at the intersection of square cavity and protruded section of inlet and outlet. These cylinders are with an equal diameter of 0.03L. The geometry of the problem recognized and represented in Fig.1 and Fig.2 (a)-(c).

Here we assume that the square block is heated at 100 degree Celcius (373 K). It is assumed that the cylinders have a heat flux of  $100 \text{ W/m}^2$ . The fluid is said to be incompressible laminar flow fluid. That is the density is constant throughout the flow. The fluid field is considered as air.

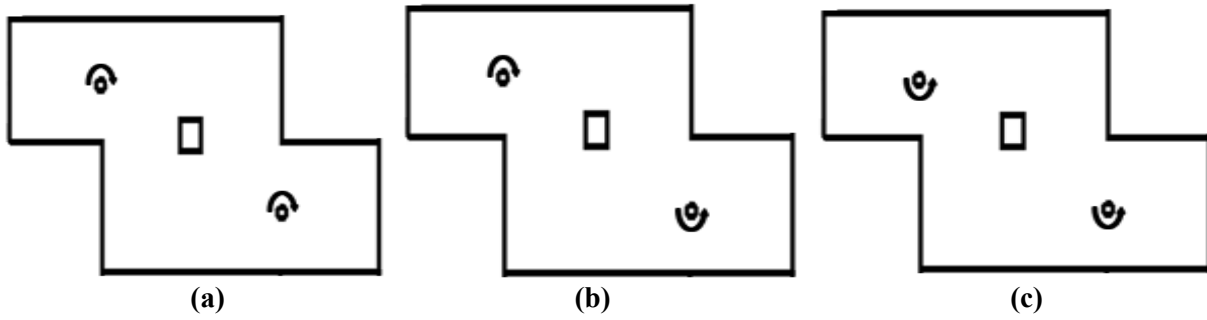


Fig.2 (a) Case1: ICW,OCW, (b) Case 2 : ICW,OACW, (c) Case 3 : IACW,OCW

## 2.1 Governing equation

The fluid flow in a square cavity can be replicated by a set of momentum and mass conservation equations. The calculations used here are Navier- Stokes equation. The continuity equation also acts as a basic for the lid driven cavity flow.

Continuity equation, (1)

$$\frac{\partial u}{\partial x} + \frac{\partial v}{\partial y} = 0$$

X- Momentum equation, (2)

$$u \frac{\partial u}{\partial x} + v \frac{\partial u}{\partial y} = -\frac{1}{\rho} \frac{\partial p}{\partial x} + \frac{\mu}{\rho} \left[ \frac{\partial^2 u}{\partial x^2} + \frac{\partial^2 u}{\partial y^2} \right]$$

Y- Momentum equation, (3)

$$u \frac{\partial v}{\partial x} + v \frac{\partial v}{\partial y} = -\frac{1}{\rho} \frac{\partial p}{\partial y} + \frac{\mu}{\rho} \left[ \frac{\partial^2 v}{\partial x^2} + \frac{\partial^2 v}{\partial y^2} \right]$$

The above equations were non- dimensionalized as follows:

$$\begin{aligned} U &= \frac{u}{U_{\infty}}; & V &= \frac{v}{U_{\infty}}; & X &= \frac{x}{L}; & Y &= \frac{y}{L}; \\ P &= \frac{P}{\rho U_{\infty}}; & Re &= \frac{U_{\infty} L}{\gamma}; & \gamma &= \frac{\mu}{\rho} \end{aligned}$$

Introducing the above non- dimensionalized (eq. 4) scales in the governing equations (eqs.1, 2, 3), we obtain the non- dimensional form of the equations as follows:

Continuity equation, (4)

$$\frac{\partial U}{\partial X} + \frac{\partial V}{\partial Y} = 0$$

X- Momentum equation, (5)

$$U \frac{\partial U}{\partial X} + V \frac{\partial U}{\partial Y} = -\frac{\partial P}{\partial X} + \frac{1}{Re} \left[ \frac{\partial^2 U}{\partial X^2} + \frac{\partial^2 U}{\partial Y^2} \right]$$

Y- Momentum equation, (6)

$$U \frac{\partial V}{\partial X} + V \frac{\partial V}{\partial Y} = -\frac{\partial P}{\partial Y} + \frac{1}{Re} \left[ \frac{\partial^2 V}{\partial X^2} + \frac{\partial^2 V}{\partial Y^2} \right]$$

The L is the reference distance dimension, while  $U_{\infty}$  is the speed with which the top lid is driven from left to right in the x- direction. The fluid property  $\gamma$  is the kinematic viscosity;  $\mu$  is the dynamic viscosity;  $\rho$  is the density of the fluid considered inside the cavity. The Reynold's number  $Re$ , is the ratio of inertial force to the viscous force, which impacts the fluid flow features in the square cavity.

The governing equations of flow and heat transfer are solved by using a finite volume solver CFX. The semi implicit method for the pressure linked equations (SIMPLE) has been used as the pressure velocity coupling scheme. The upwind scheme is employed to discretize the convective and diffusive terms. Convergences of the solution are checked by monitoring the residues of discretized governing equations. A convergence criterion of  $10^{-6}$  is used for continuity, momentum and energy equations.

Firstly, the heat transfer of the block and cylinders is analyzed for fluid flow at Reynolds number  $Re = 40$  with different non-dimensional rotational velocity range of  $0 \leq \alpha \leq 4$  and both cylinders rotating in clockwise direction. Then, the heat transfer of the block and cylinders is analyzed for two conditions, namely: Inlet cylinder rotating in clockwise direction and outlet cylinder rotating in anticlockwise direction. Inlet cylinder rotating in anticlockwise direction and outlet cylinder rotating in clockwise direction. The velocity of the fluid is calculated based on the Reynolds number ( $Re$ ) at considered ambient condition. Under the ambient condition the density ( $\rho$ ) of the air is taken as  $\rho = 1.225 \text{ kg / m}^3$  and the dynamic viscosity ( $\mu$ ) is taken as  $\mu = 1.7894 \times 10^{-5} \text{ Ns/m}^2$ . The sides of the cavity are considered as walls with the condition of no slip and stationary. The square block taken at the geometric center of the cavity is taken as a solid block with no slip and stationary wall condition. The cylinders are taken as a solid walled cylinder with no slip and moving wall condition. The moving wall has rotational motion with a varying speed ranging from  $0 \leq \alpha \leq 4$ .

Grid independency result was achieved in this study according to the procedure outlined by Freitas. Several meshes, with increasing refinement were tested to ensure that the solution was independent of mesh. We have solved the cavity with square block having rotating cylinders at inlet and outlet of the cavity with that the mesh independence of the cavity with square block for different meshes with mesh interval size of 0.01, 0.008, 0.0075, 0.006 and 0.005. The velocity profile graph (U-velocity vs. Y) was plotted. From the graph it is observed that there is a negligible change in the values of the U- velocity when plotted against the Y-axes. This shows that mesh independence of the problem considered. From the graph the mesh interval size = 0.005 to be applied in the present problem for generating more accurate and error free results.

Table 2.1: Number of nodes corresponding to the element size of the generated mesh

S.NO	Element size	Number of Nodes
1.	0.0100	77963
2.	0.0080	87963
3.	0.0075	85463
4.	0.0060	87963
5.	0.0050	92963

## 2.2 Problem Validation

As we have considered the  $AR = 1$ , take height and width of the cavity as 1.83m and at first, a square cavity is designed with the co-ordinates (0, 0) to (1.83, 1.83). Then a cylindrical element with diameter 3cm is created. This acts as the geometric center of square cavity. This geometry is used to generate surface of interest. Each edge of interest with regard to boundary conditions is named and generated. Using MESH, the created surface is subject to a default mesh, by which the square cavity is divided into a number of nodes so that the finite volume method could be applied to the cavity in order to solve the governing equation. The MESH is predefined with unstructured mesh configuration. For fine mesh, we incorporate element size of 0.005. Also for further precise results, edge refinement of value 3 is established. The final mesh being created consists of 60879 nodes. Free slip condition is imposed to the outer walls. Left wall is defined as the inlet with air as fluid field and right wall is considered as the outflow wall. Based on the values of Reynold's number, density, and dynamic viscosity values, the velocity (u velocity) is calculated for inlet fluid field for Reynold's number equals to 40. The various non dimensional angular velocities for the cylinder is defined ranging from  $0 \leq \alpha \leq 4$ . A second order upwind is used of convection to get more accurate flow results. The accuracy may also be increased by increasing the order of decimals in the residual monitors. The problem is iterated and convergence of the problem will be more accurate and error free as the level of iterations is increased and more accurately the convergence with the past results will happen.

In that there is a formation of vortices or wakes depending on the non - dimensional angular velocity of the driven lid ranging from  $0 \leq \alpha \leq 4$  and Reynold's number equals to 40. The streamline plots and contour plots for various ranges of  $\alpha$  is shown below in Fig.3 (a)-(b) and Fig.4 (a)-(e) The comparison graph plotted against local Nusselt number and various ranges of  $\alpha$  is shown in Fig 5. The resultant graph acts as validation

for our problem statement. study has been validated with the existing numerical work reported in literature [4], to investigate heat transfer from a stationary heated cylinder in cross-flow. The comparison of results of Local Nusselt number variations shown in Fig. 5 is of good agreement with each other.



**Fig.3 (a)-(b):** Stream traces ( $Re = 40, q''_{Cylinder} = 100 \text{ W/m}^2, \alpha = 1$ )

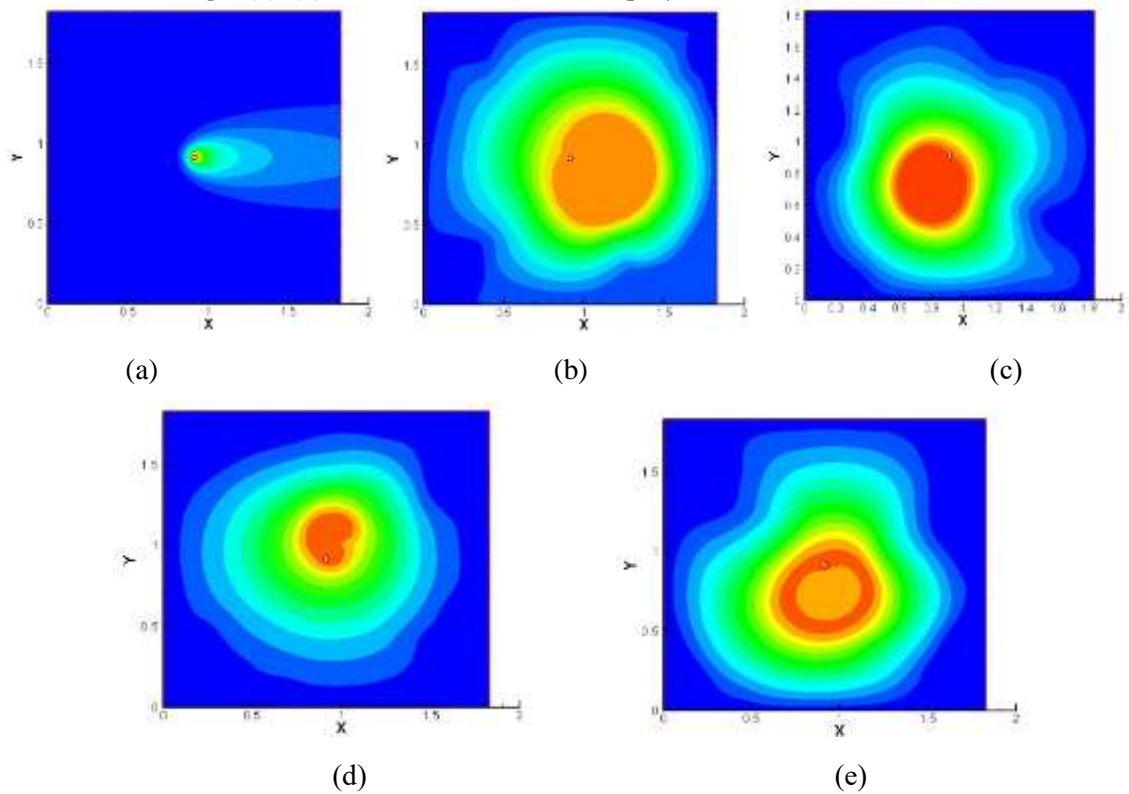


**Fig.4 (a)-(e):**  $\alpha = 0, \alpha = 1, \alpha = 2, \alpha = 3, \alpha = 4$  Isotherms ( $Re = 40, q''_{Cylinder} = 100 \text{ W/m}^2$ )

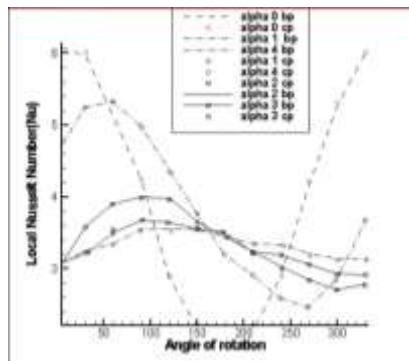


**Fig.5** Comparison of Local Nusselt number ( $Nu_L$ ) along the circumference of the cylinder for different non-dimensional rotational velocity ( $\alpha$ ). ( $Re = 40, q'' = 100 \text{ W/m}^2, Pr = 0.7$ )

### 3. Results and Discussion

Description of our problem considered is that a square cavity is considered with an aspect ratio of 1 ( $AR = H/L = 1$ ). The outflow is a protruded section taken at the bottom of the right wall which has a length  $0.5L$  and breadth of  $0.5L$ . An arrangement of events begins to develop when Reynolds number is amplified beyond 40, at which the wake behind the cylinder becomes unstable. Numerical investigation shows that wake develops a slow swaying in which the velocity is episodic in time and downstream distance. The fullness of oscillation increases downstream. The wavering wake rolls up into two staggered rows of vortices with conflicting sense of rotation. In the range  $40 < Re < 80$ , vortex street does not interact with the pair of attached vortices. As  $Re$  is increased beyond 80 the vortex street forms closer to the cylinder, and the attached eddies themselves begin to oscillate. Finally, the devoted eddies occasionally break off alternately from the two sides of the cylinder. While an eddy on one side is shed, that on the other side forms, resulting in an unsteady flow near the cylinder. As vortices of opposite circulations are shed off alternately from the two sides, the circulation around the cylinder variations sign, resulting in an wavering "lift" or lateral force. If the frequency of vortex flaking is close to the natural frequency of some mode of vibration of the cylinder body, then a considerable lateral vibration ends. To reduce the unsteady condition resulting due to increase in Reynolds number, we choose  $Re = 40$ .

#### 3.1 Interpretations based on number of vortices formed

The following figures show the results of the analysis of the problem- fluid flow and heat transfer of a square cavity with straight rotating cylinder in clockwise and anticlockwise way with a heated block in the geometric midpoint. The results are presented in the form of velocity profiles, fluid flow stream trace outlines, temperature contours and Nusselt number chart. These results are presented for three different cases.

Case (i): The results are plotted for the problem first by varying the non-dimensional rotational velocity of the rotating cylinder. Here the fluid flowing into the cavity is for a constant Reynolds number 40. Direction of rotation for both cylinders are in same that is clockwise direction.

Case (ii): The results are plotted for the problem first by varying the non-dimensional rotational velocity of the rotating cylinder. Here the fluid flowing into the cavity is for a constant Reynolds number 40. Direction of rotation for inlet cylinder is clockwise and outflow cylinder is anticlockwise direction.

Case (iii): The results are plotted for the problem first by varying the non-dimensional rotational velocity of the rotating cylinder. Here the fluid flowing into the cavity is for a constant Reynolds number 40. Direction of rotation for inlet cylinder is anticlockwise and outflow cylinder is clockwise direction.

In Fig.6 (a)-(i) shows the stream contours for the non-dimensional rotational velocity considered ( $\alpha=0,1,2,3,4$ ). In this case the direction of rotation for both cylinders is clockwise. The stream contours depict the nature of the flow commencing inside the cavity, the effect of the presence of the square solid block is placed center of the cavity and rotating cylinders placed at the inlet and outflow on the flow field. This also gives the details about the formation of the primary vortex (also known as wakes) and the other corner vortices due to the flow field. These vortices were formed due to the presence of low pressure at the corners. The Fig.6 (j) - (o) shows the stream contours for the non-dimensional rotational velocity considered ( $\alpha=0,1,2,3,4$ ). In this case the direction of rotational for inlet cylinder is clockwise and outflow cylinder is anticlockwise. The stream contours depict the nature of the flow commencing inside the cavity, the effect of the presence of the square solid block at the geometric center of the cavity and rotating cylinders placed at the inlet and outflow on the flow field. This also gives the details about the formation of the primary vortex and the other corner vortices due to the flow field. These vortices were formed due to the presence of pressure variations at the corners.

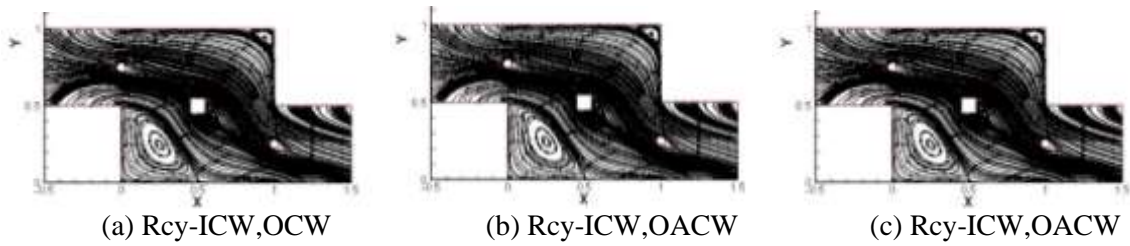


**Fig.6 (a)-(c):** Stream traces ( $Re = 40, T_{block}=373 \text{ k}, q''_{Cylinder} = 100 \text{ W/m}^2, \alpha=0$ )

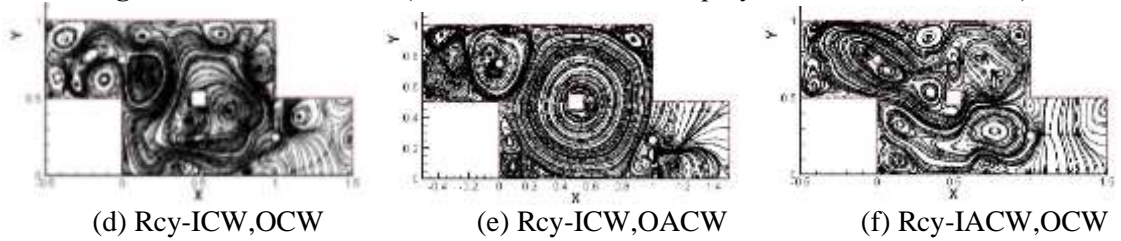


**Fig.6 (d)-(f):** Stream traces ( $Re = 40, T_{block}=373 \text{ k}, q''_{Cylinder} = 100 \text{ W/m}^2, \alpha=1$ )

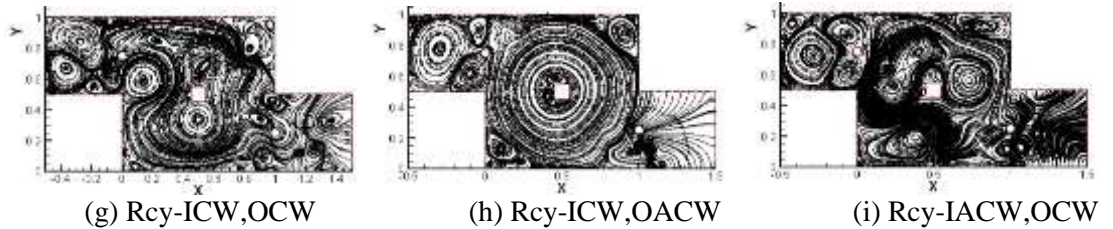


**Fig.6 (g)-(i):** Stream traces ( $Re = 40, T_{block}=373 \text{ k}, q''_{Cylinder} = 100 \text{ W/m}^2, \alpha=2$ )

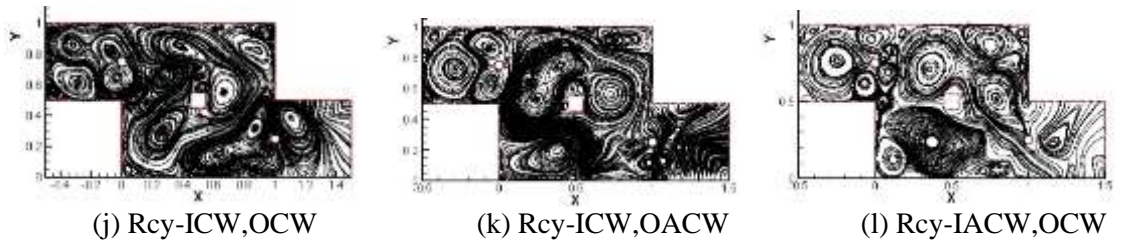


**Fig.6 (j)-(l):** Stream traces ( $Re = 40, T_{block}=373 \text{ k}, q''_{Cylinder} = 100 \text{ W/m}^2, \alpha=3$ )

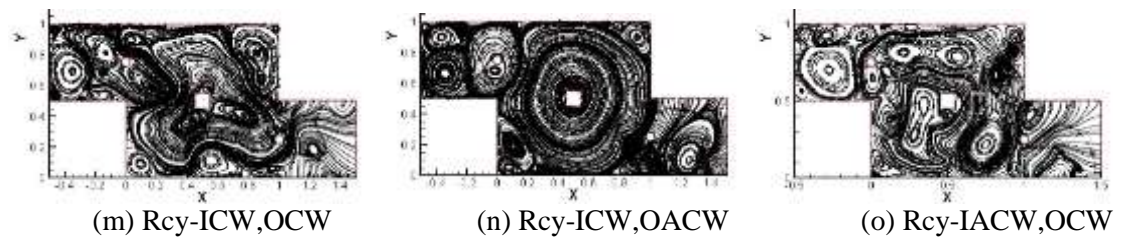


**Fig.6 (m)-(o):** Stream traces ( $Re = 40, T_{block}=373 \text{ k}, q''_{Cylinder} = 100 \text{ W/m}^2, \alpha=4$ )

The Fig.7 (a) – (j) shows the temperature contours for different non-dimensional rotational velocities of the rotating cylinder in the cavity for  $\alpha = 0, 1, 2, 3, 4$  and different combinations of direction of rotation of cylinder. The temperature contour explains the heat transfer that takes place between the fluid flow field, rotating cylinder and the heated solid square block at the different zones in the cavity. This helps to visualize the heat transferred to the fluid, maximum and minimum temperature of the fluid field inside the cavity and the effective heat transfer for different non-dimensional rotational velocity with predetermined direction of rotation of cylinder and the effect of varying the non-dimensional rotational velocity with change in direction of rotation on the heat transfer.

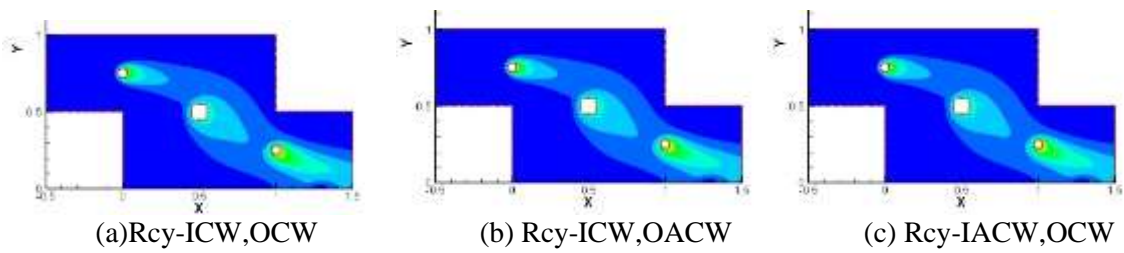


**Fig.7(a)-(c): Isotherms (Re = 40, Tblock=373 k, q''Cylinder = 100 W/m<sup>2</sup>,  $\alpha = 0$ )**

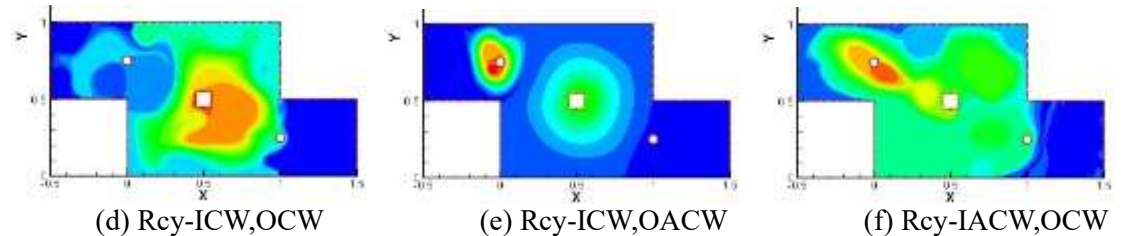


**Fig.7 (d)-(f): Isotherms(Re = 40, Tblock=373 k, q''Cylinder = 100 W/m<sup>2</sup>,  $\alpha = 1$ )**

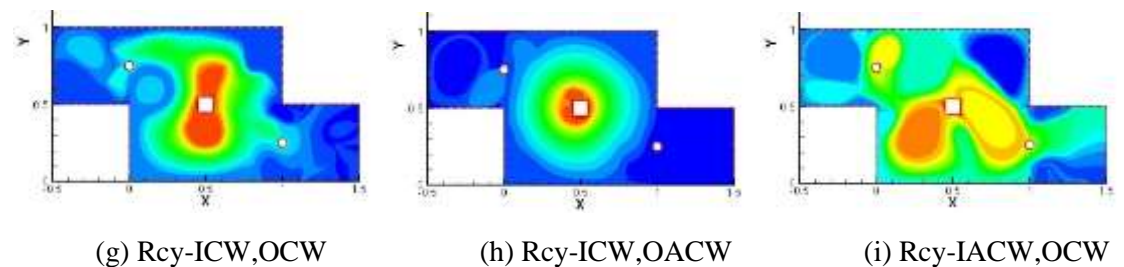


**Fig.7 (g)-(i): Isotherms(Re = 40, Tblock=373 k, q''Cylinder = 100 W/m<sup>2</sup>,  $\alpha=2$ )**

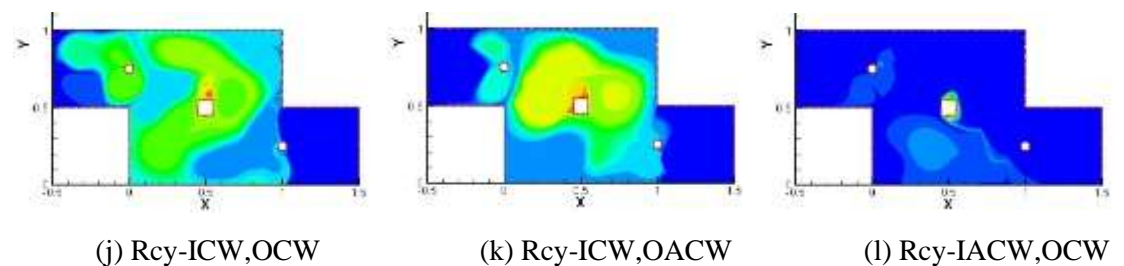


**Fig.7 (j)-(l): Isotherms(Re = 40, Tblock=373 k, q''Cylinder = 100 W/m<sup>2</sup>,  $\alpha = 3$ )**

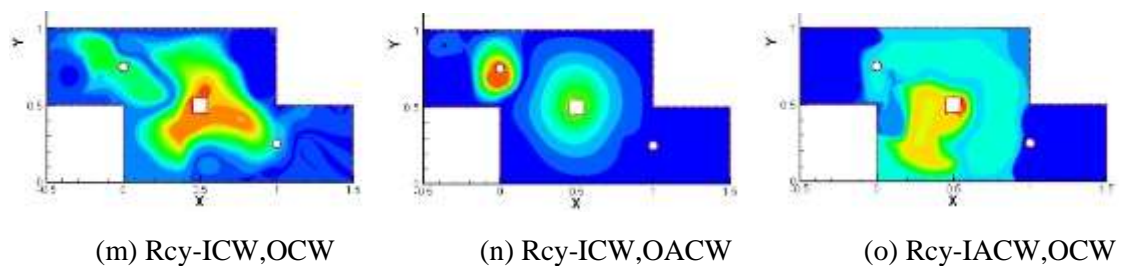


**Fig.7 (m)-(o): Isotherms(Re = 40, Tblock=373 k, q''Cylinder = 100 W/m<sup>2</sup>,  $\alpha=4$ )**

A vortex (plural vortices) is a rapidly spinning, circular or spiral flow of fluid around the central axis. The swirling motion tends to suck everything within the fluid toward its center. The speed and rate of rotation of the fluid are greatest at the center, and decrease progressively with distance from the center. This phenomenon takes place due adverse pressure gradient, change in Nusselt number(Nu), change in Reynolds number and geometry through which the fluid flows.

Table 3.1 Number of secondary vortices formed with respect to each  $\alpha$

Non-dimensional rotational velocity( $\alpha$ )	ICW, OCW	ICW, OACW	IACW, OCW
0	3	3	3
1	19	19	21
2	23	20	23
3	25	24	25
4	26	18	27

Table 3.2 Vortex position and size with respect to various non-dimensional rotational velocity ( $\alpha$ )

Non-dimensional rotational velocity( $\alpha$ )	ICW,OCW			ICW,OACW			IACW,OCW		
	Vortex position		Vortex size	Vortex position		Vortex size	Vortex position		Vortex size
	X_Coor (m)	Y_Coor(m)	(m)	X_Coor(m)	Y_Coor (m)	(m)	X_Coor(m)	Y_Coor(m)	(m)
0	0.25559	0.24076	0.4800	0.25559	0.24076	0.48000	0.25559	0.24076	0.48000
1	0.56091	0.54900	1.2450	0.55219	0.53164	1.11540	0.56091	0.54900	1.24500
2	0.55655	0.50993	1.3259	0.44604	0.54202	1.15600	0.45623	0.44915	1.24980
3	0.55219	0.56203	1.0069	0.55701	0.51000	1.00500	0.55655	0.70529	1.00438
4	0.46931	0.56637	1.3290	0.55802	0.50149	0.95005	0.33846	0.37535	0.64216

From Table 3.2, we observe that constant vortices formation takes place when  $\alpha = 2$ . till  $\alpha = 1$ , vortices formation is not constant. This is due to the fact that fluid flow is not obstructed rotational speed of cylinder; hence backflows are reduced.

#### 4. Conclusion

The present study highlights the features of fluid flow and heat transfer in a square cavity with flat revolving cylinder in clockwise and anticlockwise path with a heated block in the geometric midpoint. The study includes the investigation of the fluid field flow nature, primary vortices, secondary vortices, the heat transfer of the heated block for dissimilar non dimensional rotational velocities ( $\alpha=0,1,2,3$  and 4). The examination is also deliberate for combinatorics of direction of the rotation of the cylinder. From Table 3.1, we realize that amount of vortices decrease slowly till  $\alpha =3$ . This is due to the fluid gesture being liberated by wakes. At  $\alpha = 4$ , the number of vortices formed rises with a similar value of total vortices formed at  $\alpha = 2$ . This can be due to augmented wake formation around the cylinder.  $\alpha = 3$  acts as the inflationary point for number of vortices formed. Hence, we reflect  $\alpha = 3$  as the critical non-dimensional rotating speed.

## Nomenclature

Symbol	Quantity	Symbol	Quantity
$C_p$	specific heat of fluid (J/kg K)	$T$	Temperature (K)
$D$	diameter of the circular cylinder (m).	$T_\infty$	Temperature of fluid at inlet (K).
$h$	local convective heat transfer coefficient. (Wm <sup>-2</sup> K <sup>-1</sup> ).	$U$	Velocity vector.
$k$	thermal conductivity of fluid (W/m K)	$U_\infty$	Uniform velocity of fluid at inlet (ms <sup>-1</sup> ).
$L_1$	upstream length from the inlet to the centre of the cylinder (m)	$u$	x-component of velocity(ms <sup>-1</sup> ).
$L_2$	downstream length from the centre of the cylinder to the outlet (m)	$v$	y component of velocity(ms <sup>-1</sup> ).
$L_y$	height of the computational domain (m)	<b>Greek letters</b>	
$Nu_L$	local Nusselt number.	$\alpha$	Non-dimensional rotational velocity.
$Nu_{avg}$	mean Nusselt number.	$\nu$	Kinematic viscosity (m <sup>2</sup> /s).
$P$	pressure (Pa)	$\rho$	Density (kgm <sup>-3</sup> ).
$Pr$	Prandtl number.	$\Omega$	Angular velocity (rads <sup>-1</sup> ).
$q''$	heat flux (Wm <sup>-2</sup> ).	$\theta$	Angular displacement from the front stagnation point in the anti-clockwise direction (degrees).
$Re$	Reynolds number ( $U_\infty D/\nu$ ).		

## REFERENCES

- [1]. Shankar P.M. Fluid mechanics in the driven cavity. Annual Review of Fluid Mechanics, 32(1), 93-136
- [2]. Ghasemi B., & Aminossadati S. M. Mixed convection in a lid-driven triangular enclosure filled with nanofluids. International Communications in Heat and Mass Transfer, 37(8), 1142-1148.
- [3]. S.Rakesh S., Kanna, P.R, Numerical investigation of flow and heat transfer from a block placed in a cavity subject to different inlet conditions- Velammal College of Engineering and Technology.
- [4]. Prabul Chandra, H.AbdulJaleel, Laminar Forced Convection from a Rotating Horizontal Cylinder in Cross Flow” College of Engineering.
- [5]. A.J. Chamkha, Hydromagnetic combined convection flow in a vertical lid- driven cavity with internal heat generation or absorption, Numer. Heat Transfer, Part A, vol. 41, pp.529-546.
- [6]. Chen S, A large-eddy-based lattice Boltzmann model for turbulent flow simulation. Applied Mathematics and Computation, 215, 591–595.
- [7]. C.M. Cheng, Y.Y.Chen. Numerical simulation and validation of wind load and structural responses of an isolated tall building in turbulent boundary layer flow, The Fifth International Symposium on Computational Wind Engineering, USA May 23-27.
- [8]. Ercan Erturk, Turkey, Discussion on driven cavity flow, Int. J. Numerical Meth. Fluids: vol60: pp. 275- 294.
- [9]. M.L. Facchinetti, F. Biolley, Coupling of structure and wake oscillators in vortex-induced vibrations. Journals of fluid and structures, 19 (3): 123-140
- [10]. Fudhail et al. Numerical simulation of flow behavior in driven cavity at high Reynolds number, IIUM Engg. Journal, Vol. 12 No. 6
- [11]. G. Gau Mixed convection in rectangular cavities at various aspect ratios with moving isothermal side walls and constant flux heat source on the bottom wall Int. J. Therm. Sci., 43, pp. 465–475.
- [12]. U. Ghia, High- Re solutions for incompressible flow using Navier- Stokes equation and Multigrid method, Journal of Physics: 387- 411.
- [13]. K.M. Khanafer, Numerical simulation of unsteady mixed convection in a driven cavity using an externally excited sliding lid, European J. Mechanics B/Fluids, vol. 26, pp.669-687.

- [14]. J. M. Khodadadi, fluid flow and heat transfer in a lid-driven cavity due to an oscillating thin fin: Transient behavior, *Journal of Heat transfer*, ASME, Vol.126.
- [15]. G. Iaccarino, A. Ooi, M. Behnia. (2003) Reynolds Averaged Simulation of unsteady separated flow [J]. *Journal of Heat and Flow*, 24,147-156.
- [16]. Lam k, Gong w q, Numerical simulation of cross-flow around four cylinders in an in-line square configuration. *Journal of Fluid and Structures*, 24(I): 34-57
- [17]. E. de Langre, Frequency lock-in is caused by coupled-mode flutter. *Journals of fluid and structures* , 22: 783-791
- [18]. S.L. Li, Y.C. Chen, Multi relaxation time lattice Boltzmann simulations of deep lid driven cavity flows at different aspect ratios. *Comput. & Fluids*, 2011, 45(1): 233- 240.
- [19]. Manab kumar Das, P.Rajesh Kanna, *Int. J. Numerical method for Heat transfer and Fluid flow*, Vol. 7 No. 8,: pp. 799- 822.
- [20]. O. Manca, S. Nardini, Effect of Heated Wall Position on Mixed Convection in a Channel with an Open Cavity, *Numer. Heat Transfer, Part A*, vol. 43, pp.259–282.
- [21]. S. Manzoor, P. Hernon Vibrations of a square cylinder in a wind tunnel, 3'd Fluids Engineering Summer Meeting, Canada.
- [22]. C. Migeon, and A. Texier, Three-dimensionality development inside standard parallel pipe lid-driven cavities at  $Re = 1000$ . *J. Fluids and Struc.*, 17 (1): 717–738. Ch.-H. Bruneau, M. Saad, The 2D lid-driven cavity problem revisited, *Computers & Fluids*35 (3).
- [23]. Reyad Omari, CFD simulation of lid driven cavity flow at moderate Reynolds number, *Jordan, European scientific journal*, ISSN: 1857- 7881
- [24]. P. N. Shankar, M. D. Deshpande, *Annu. Rev. Fluid Mech.* 2000.32:93-136. Downloaded from arjournals. annualreviews.org by NATIONAL AEROSPACE LABS on.
- [25]. N.A. C. Sidik and S. M. R. Attarzadeh, An accurate numerical prediction of solid particle fluid flow in a lid-driven cavity. *Intl. J. Mech.*, 5(3): 123-128.
- [26]. Song Chongfang, Dong Lei, Peng Lin. Numerical Simulation of unsteady flow around an environmental square cylinder, *College of Environment Science and Engineering*.